JOURNAL OF GUIDANCE, CONTROL, AND DYNAMICS
Vol. 25, No. 3, May–June 2002

Desensitized Jerk Limited-Time Optimal Control of Multi-Input Systems

Marco Muenchhof* and Tarunraj Singh†
State University of New York at Buffalo, Buffalo, New York 14260

The problem of designing jerk limited-time optimal control profiles for rest-to-rest maneuvers of flexible structures with multiple actuators is addressed. The problem formulation includes constraints to cancel the poles corresponding to the rigid-body mode and flexible modes of the system and to satisfy the boundary conditions of the rest-to-rest maneuver. Further constraints can be added to increase robustness to parametric uncertainties of the plant. The technique proposed is applied to a three-mass/two-spring system and the evolution of the shape of the control profile as a function of jerk is illustrated.

I. Introduction

THERE has been extensive research in the field of vibration control of slewing flexible structures. The knowledge obtained throughout this research has been applied to a wide variety of control problems, including, but not limited to, maneuvering of large space structures,[1] flexible arm robots,[2] computer disk drives,[3] and cranes.[4] In most of these applications, the objective of the controller is to minimize the maneuver time with quiescent final states. Robustness to modeling errors, limits on fuel consumed, maximum deformation permitted, and so on, have been included in the problem formulation as additional constraints.

Research in the field of input shaping was motivated by Smith's development of the Posicast Control.[5] The sensitivity of these controllers to uncertainties in damping and frequencies of the modes was addressed by Singer and Seering,[6] and the resulting prefilter was referred to as an input shaper. Singh and Vadali[7] illustrated that a time-delay prefilter that cancels the underdamped poles of the system results in the same control profile as the input shaped controller. They also illustrated that the use of a series of time-delay filters results in increased robustness to modeling errors. Various other approaches, which include forcing the derivative of the sensitivity curve at the nominal values of the model parameters to zero and designing input shapers that maximize the uncertain region where the residual vibration is less than a prespecified quantity,[8] have been investigated in the interest of desensitizing the prefilter with respect to modeling errors. Techniques to desensitize the time-optimal control profile have been developed by Liu and Wie[9] and Singh and Vadali.[10] A very recent approach to the design of desensitized time-delay filters is a minimax formulation proposed by Singh.[11] All of the aforementioned approaches assume that the actuator can track step inputs, which is equivalent to requiring infinite jerk control profiles. Jerk is indicative of the time rate of change of the inertia forces and is a measure of the impact levels that can excite unmodeled dynamics, which is of concern in the control of flexible structures. Bhat and Miu[3] study the problem of designing control profiles, minimizing a cost function that is the time integral of the square of the absolute magnitude of the instantaneous jerk. Hindle and Singh[12] reformulated the problem as the minimization of a weighted combination of the jerk and the power consumed. They also proposed using the state-sensitivity equations to arrive at control profiles that are insensitive to modeling errors. Both of these approaches do not account for finite limits on the control or the jerk.

Thus far, little research has been carried out in the field of input prefilter design for multi-input systems. In this field of application, it is usually necessary to cancel multiple oscillatory modes. Singh and Vadali[13] presented the design of input prefilters for multimode single-input systems. An arbitrary number of pole cancellation constraints can be introduced, which means that the algorithm is limited neither in the number of modes, nor in the desired level of robustness. The designer has the latitude to select the sampling time or to constrain the magnitude of the input sequence. The latter is interesting because small sampling times can lead to undesirable large control inputs. The design method was presented for single-input systems. It can be extended to multi-input systems by designing a filter for each input separately. Each filter would be required to cancel all poles of the system, which might be redundant and results in long maneuver times.

Lim et al.[14] presented a dynamic optimization-based control design algorithm for multi-input systems. This algorithm calculates the amplitude profile of a discrete-time control sequence. A variety of constraints can be added to the optimization statement. These constraints include limits on the magnitude of the time rate of change of the input sequence, as well as state and transient response constraints. Increased robustness is achieved by evaluating the objective function and constraints, not only for the nominal system, but also for a number of perturbed systems. The entire algorithm is composed of two steps: First, the minimal filter length is determined. Then, the optimizer solves for the shape of the control inputs.

Pao[15] extended the pole cancellation approach to multi-input systems. By solving for all input shapers simultaneously, the filter length can be reduced compared to the case where the input shaping filters are designed for each input separately.

This paper is concerned with the design of time-optimal control profiles for multi-input systems. Constraints on the maximum magnitude of jerk are introduced. The proposed technique is illustrated on a three-mass/two-spring system, undergoing a rest-to-rest maneuver. Even though a two-input systems with two flexible modes has been chosen for the numerical examples presented in this paper, it must be emphasized that the algorithm is neither limited in the number of inputs, nor in the number of modes. To account for the constraints imposed on the jerk, new states are introduced into the system model. These new states represent the control inputs. The time rate of change of the control input, that is, the jerk, will now represent the input driving the augmented system.

Received 8 March 2001; revision received 28 September 2001; accepted for publication 2 October 2001.

*Graduate Student, Department of Mechanical and Aerospace Engineering; currently, Graduate Student, University of Technology at Darmstadt, Institute of Automatic Control, Laboratory of Control Systems and Process Automation, Darmstadt, 64283 Germany.

†Associate Professor, Department of Mechanical and Aerospace Engineering.

II. Problem Formulation

The performance index for the time-optimal control is given by

$$F = \tfrac{1}{2}T_{\text{final}}^2 \tag{1}$$

where T_{final} is the maneuver time. The equations of motion of an undamped mechanical system with p inputs are given by a set of m second-order differential equations of the form

$$M\ddot{\boldsymbol{y}}(t) + K\boldsymbol{y}(t) = D\boldsymbol{u}(t) \tag{2}$$

where M and K represent the mass and stiffness matrices, respectively. D, the control input matrix, is a function of the location of the actuators. The bounds on the time rate of change of the control inputs are imposed in the form

$$-J \le \dot{u}_k(t) \le J \qquad \forall\, k \in \{1, 2, \ldots, p\}\ \forall\, t \tag{3}$$

The control inputs themselves have the limits

$$-1 \le u_k(t) \le 1 \qquad \forall\, k \in \{1, 2, \ldots, p\}\ \forall\, t \tag{4}$$

Furthermore, for the desired rest-to-rest maneuver of unit length, the boundary conditions

$$\begin{aligned} y_i(0) &= 0 \qquad & y_i(T_{\text{final}}) &= 1 \\ \dot{y}_i(0) &= 0 \qquad & \dot{y}_i(T_{\text{final}}) &= 0 \qquad \forall\, i \in \{1, 2, \ldots, m\} \\ \ddot{y}_i(0) &= 0 \qquad & \ddot{y}_i(T_{\text{final}}) &= 0 \end{aligned} \tag{5}$$

have to be satisfied. These bounds have been imposed without a loss of generality. Other constraints on $|u_k(t)|$ and $y_i(T_{\text{final}}) = y_{i,\text{final}}$ can be realized by scaling the system matrices accordingly.

III. Parameterization of the Control Profiles

The time-optimal/jerk-limited control profiles will be realized by superposing time-delayed ramp functions with different slopes. This will be discussed in Sec. IV.D. Time optimality requires that all $u_k(t), k \in \{1, 2, \ldots, p\}$, are in saturation for as much time as possible. However, constraining the jerk [Eq. (3)] might prevent $u_k(t), k \in \{1, 2, \ldots, p\}$, from saturating because the switching times could be closer than the minimum distance needed to saturate the control input. Additionally, it is required that all inputs be switched off at the same final time T_{final}.

For the following derivation, the control profiles will be parameterized by the switching times for the given input sequences as shown in Fig. 1. The different control input sequences are given as

$$u_k(t) = J\left(\sum_{j=1}^{n_k} A_{k,j}\langle t - T_{k,j}\rangle\right) \tag{6}$$

with a time rate of change of

$$\dot{u}_k(t) = J\left(\sum_{j=1}^{n_k} A_{k,j}\mathcal{H}(t - T_{k,j})\right) \tag{7}$$

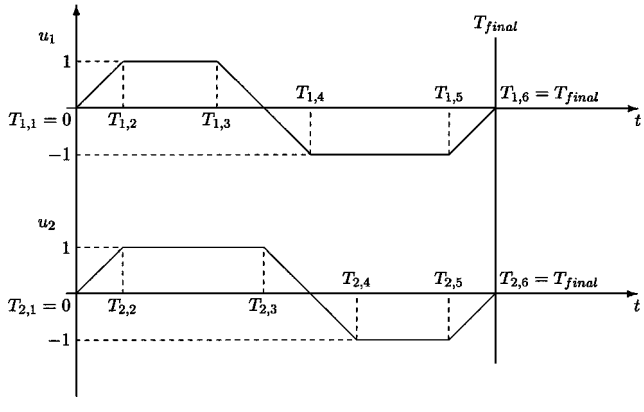

Fig. 1 Parameterization of the control profiles for multi-input systems.

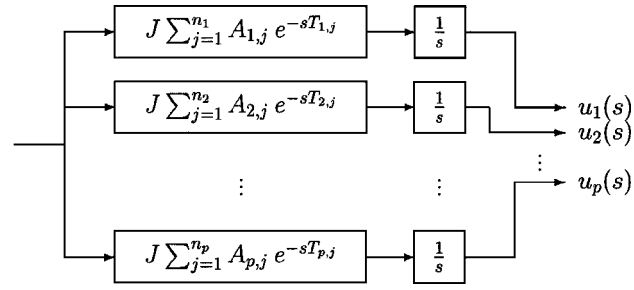

Fig. 2 Structure of the time-delay filtering controller.

where $\mathcal{H}(x)$ denotes the unit-step (Heaviside) function, $\langle x\rangle = x\mathcal{H}(x)$,

$$T_{k,n_k} = T_{\text{final}} \qquad \forall\, k \in \{1, 2, \ldots, p\} \tag{8}$$

and $n_k - 2$ is equivalent to the number of switches in the control sequence applied at input k. The coefficients $A_{k,j}$ are restricted by

$$\begin{aligned} A_{k,j} &\in \{-2, -1, 1, 2\} \qquad \forall\, k \in \{1, 2, \ldots, p\} \\ j &\in \{2, 3, \ldots, n_k - 1\} \end{aligned} \tag{9}$$

For the first switch in each control sequence, that is, $j = 1$,

$$A_{k,1} \in \{-1, 1\} \qquad T_{k,1} = 0 \qquad \forall\, k \in \{1, 2, \ldots, p\} \tag{10}$$

This means that all input sequences start at $t = 0$. For the last amplitude in each sequence, that is, $j = n_k$,

$$A_{k,n_k} \in \{-1, 1\} \qquad \forall\, k \in \{1, 2, \ldots, p\} \tag{11}$$

The initial input can be either positive or negative depending on the desired maneuver.

The control profiles are generated by a feedforward controller that is composed of time-delay filters and integrators. There is a separate time-delay filter for each input. Each filter is driving an integrator, which, in turn, feeds the corresponding system input. The resulting structure of the controller is shown in Fig. 2.

IV. Parameter Optimization

In this section, analytical equations will be derived that lead to control sequences for rest-to-rest maneuvers of undamped flexible structures with multiple resonant modes and multiple inputs. Only multi-input systems whose behavior can be described by the state-space equations

$$\dot{\boldsymbol{x}}(t) = Q\boldsymbol{x}(t) + R\boldsymbol{u}(t) \qquad y_O(t) = S_O x(t) \tag{12}$$

are considered. It is assumed that there is no direct feedthrough. A direct feedthrough, if present, would not cause residual vibration for input sequences of finite length and can, therefore, be eliminated from the system. Furthermore, it is assumed that Q can be decomposed as

$$Q = \begin{bmatrix} Q_{D,0} & & & & \\ & Q_{D,1} & & & \\ & & Q_{D,2} & & \\ & & & \ddots & \\ & & & & Q_{D,(m-1)} \end{bmatrix} \tag{13}$$

where $Q_{D,i}$, $i = 0, 1, \ldots, (m-1)$, denote block matrices on the diagonal of Q. The index 0 corresponds to the rigid-body mode associated with the block matrix

$$Q_{D,0} = \begin{bmatrix} 0 & 1 \\ 0 & 0 \end{bmatrix} \tag{14}$$

It is assumed that the system is undamped, for which case the submatrix $Q_{D,i}$ is

$$Q_{D,i} = \begin{bmatrix} 0 & 1 \\ -\omega_i^2 & 0 \end{bmatrix} \tag{15}$$

and describes the dynamics of the ith flexible mode characterized by the natural frequency ω_i. The input distribution matrix R will be decomposed as

$$R = \begin{bmatrix} R_0 \\ R_1 \\ R_2 \\ \vdots \\ R_{m-1} \end{bmatrix} \tag{16}$$

where the submatrices R_i, $i = 0, 1, 2, \ldots, (m-1)$, are all of the form

$$R_i = \begin{bmatrix} 0 & 0 & \ldots & 0 \\ D_{i,1} & D_{i,2} & \ldots & D_{i,p} \end{bmatrix} \tag{17}$$

This representation of Q and R can be derived directly from the second-order system of differential equations used to describe the behavior of the mechanical system.

The transfer function matrix can be written as

$$G(s) = S_O(sI - Q)^{-1}R \tag{18}$$

where s is the Laplace variable. To calculate the inverse $(sI - Q)^{-1}$, that

$$Q = \begin{bmatrix} Q_1 & 0 \\ 0 & Q_2 \end{bmatrix} \longrightarrow f(Q) = \begin{bmatrix} f(Q_1) & 0 \\ 0 & f(Q_2) \end{bmatrix} \tag{19}$$

can be exploited because Q is of block diagonal form. The inverse of $(sI - Q)$ can be calculated blockwise.

An equation for the Laplace transform of the states associated with a given submatrix $Q_{D,i}$ can be derived as

$$\begin{aligned} X_i(s) &= (sI - Q_{D,i})^{-1}R_i\boldsymbol{U}(s) \\ &= \frac{1}{s^2 + \omega_i^2}\begin{bmatrix} s & 1 \\ -\omega_i^2 & s \end{bmatrix}\begin{bmatrix} 0 & 0 & \ldots & 0 \\ D_{i,1} & D_{i,2} & \ldots & D_{i,p} \end{bmatrix}\boldsymbol{U}(s) \end{aligned} \tag{20}$$

where $X_i(s)$ designates the Laplace transform of the aforementioned states and $\boldsymbol{U}(s)$ is a vector containing the Laplace transforms of the input signals. For the controller presented in this paper, $\boldsymbol{U}(s)$ is given as

$$\boldsymbol{U}(s) = \begin{bmatrix} J\dfrac{1}{s}\displaystyle\sum_{j=1}^{n_1} A_{1,j}e^{-sT_{1,j}} \\ J\dfrac{1}{s}\displaystyle\sum_{j=1}^{n_2} A_{2,j}e^{-sT_{2,j}} \\ \vdots \\ J\dfrac{1}{s}\displaystyle\sum_{j=1}^{n_p} A_{p,j}e^{-sT_{p,j}} \end{bmatrix} U^*(s) \tag{21}$$

where $U^*(s)$ designates the signal used to drive the time-delay filter structure, which will be a unit step. The Laplace transform of the output of the system $Y_O(s)$ is given by

$$\boldsymbol{Y}_O(s) = S_O(sI - Q)^{-1}R\boldsymbol{U}(s) = S_O X(s) \tag{22}$$

Because the output distribution matrix S_O solely consists of real numbers, each output will be a linear combination of states x_i, $i \in \{0, 1, \ldots, (m-1)\}$. Thus, if the states do not exhibit residual vibration, no output will show residual vibration. As follows, methods will be derived that eliminate residual vibration for the states x_i. The Laplace transform of the states $X_i(s)$ evaluates to

$$X_i(s) = \frac{1}{s^2 + \omega_i^2}\begin{bmatrix} 1 \\ s \end{bmatrix} J\sum_{k=1}^{p}\left(\frac{1}{s}D_{i,k}\sum_{j=1}^{n_k} A_{k,j}e^{-sT_{k,j}}\right)U^*(s) \tag{23}$$

allowing for isolating a transfer function describing how the entire time-delay filter structure acts on a certain mode. For the ith mode, this transfer function is defined as

$$G_{F,i}(s) = J\sum_{k=1}^{p} D_{i,k}\left(\sum_{j=1}^{n_k} A_{k,j}e^{-sT_{k,j}}\right) \tag{24}$$

The integrators associated with the system inputs are now treated as being part of the plant. Therefore, the integrator transfer function $1/s$ is not present in Eq. (24).

A. Cancellation of the Poles of the Oscillatory Modes

To inhibit residual vibration after the end of the maneuver for a given modal frequency, the pair of poles corresponding to that frequency have to be canceled by a pair of zeros. These zeros have to be introduced by the time-delay filter structure. This is stated as

$$G_{F,i}(s)|_{s=\pm j\omega_i} = 0 \tag{25}$$

For each mode, there will be two constraints, forcing both the real and the imaginary part of Eq. (25) to zero. Because all oscillatory poles have to be eliminated, a total of $2m-2$ constraints have to be imposed. The entire set of constraint equations is given as

$$\begin{bmatrix} \displaystyle\sum_{k=1}^{p} D_{i,k}\left(\sum_{j=1}^{n_k} A_{k,j}\cos(\omega_i T_{k,j})\right) = 0 \\ \displaystyle\sum_{k=1}^{p} D_{i,k}\left(\sum_{j=1}^{n_k} A_{k,j}\sin(\omega_i T_{k,j})\right) = 0 \end{bmatrix}$$

$$\forall\, i \in \{1, 2, \ldots, (m-1)\} \tag{26}$$

A time-delay filter structure satisfying Eq. (26) will cancel all oscillatory poles of the system and will, thus, eliminate residual vibration entirely.

B. Cancellation of the Poles of the Rigid-Body Mode

The controller has to cancel a total of three poles at the origin of the s plane. Two poles correspond to the rigid-body mode of the structure, whereas the third pole cancellation constraint was imposed to account for the added integrator in each input path. As was shown in the literature,[7,10] placing more than one zero at a certain point in the s domain is tantamount to forcing partial derivatives of the transfer function with respect to s to zero. Because three zeros have to be placed at the origin of the s plane, $G_{F,0}(s)$ must satisfy the set of constraints

$$G_{F,0}(s)|_{s=0} = 0 \qquad \left.\frac{\partial G_{F,0}(s)}{\partial s}\right|_{s=0} = 0 \qquad \left.\frac{\partial^2 G_{F,0}(s)}{\partial s^2}\right|_{s=0} = 0 \tag{27}$$

The set of equations as given in Eq. (27) will now be evaluated for the transfer function of the time-delay filter that was derived earlier. This results in

$$\begin{bmatrix} \displaystyle\sum_{k=1}^{p} D_{0,k}\left(\sum_{j=1}^{n_k} A_{k,j}\right) = 0 \\ \displaystyle\sum_{k=1}^{p} D_{0,k}\left(\sum_{j=1}^{n_k} -T_{k,j}A_{k,j}\right) = 0 \\ \displaystyle\sum_{k=1}^{p} D_{0,k}\left(\sum_{j=1}^{n_k} T_{k,j}^2 A_{k,j}\right) = 0 \end{bmatrix} \tag{28}$$

A constraint equation has to be imposed to restrict the final displacement. For the decoupled system, the final displacement is determined by the rigid-body mode dynamics only. The differential equations

$$\dot{\boldsymbol{x}}_0(t) = \begin{bmatrix} 0 & 1 \\ 0 & 0 \end{bmatrix} \boldsymbol{x}_0(t) + \begin{bmatrix} 0 & 0 & \dots & 0 \\ D_{0,1} & D_{0,2} & \dots & D_{0,p} \end{bmatrix} \boldsymbol{u}(t) \tag{29}$$

result in the constraint

$$\boldsymbol{x}_0(t)|_{t=T_{\text{final}}} = \sum_{k=1}^{p} D_{0,k} \left[\sum_{j=1}^{n_k} A_{k,j} \frac{J}{6} (T_{\text{final}} - T_{k,j})^3 \right] = \boldsymbol{x}_{0,\text{final}} \tag{30}$$

for the final displacement.

C. Constraints Accounting for the Integrators

After the end of the maneuver, no control input should be acting on the system. This is stated as

$$u_k(t) = 0 \qquad \forall\, t \geq T_{\text{final}} \qquad \forall\, k \in \{1, 2, \dots, p\} \tag{31}$$

The system is fed by integrators, which are driven by a time-delay filter structure. Two constraints must be imposed to ensure that the input $u_k(t)$ is zero for all $t \geq T_{\text{final}}$. The first constraint is given as

$$\dot{u}_k(t) = J \sum_{j=1}^{n_k} A_{k,j} \mathcal{H}(t - T_{k,j}) = 0 \qquad \forall\, t \geq T_{\text{final}} \tag{32}$$

and the second constraint is

$$u_k(t) = J \sum_{j=1}^{n_k} A_{k,j} \langle t - T_{k,j} \rangle = 0 \qquad \forall\, t \geq T_{\text{final}} \tag{33}$$

These constraints have to be imposed on every input. This leads to the set of constraint equations

$$\begin{bmatrix} \displaystyle\sum_{j=1}^{n_k} A_{k,j} = 0 \\ \displaystyle\sum_{j=1}^{n_k} A_{k,j} (T_{\text{final}} - T_{k,j}) = 0 \end{bmatrix} \qquad \forall\, k \in \{1, 2, \dots, p\} \tag{34}$$

which render the first two constraints given in Eq. (28) redundant.

D. Proof of Time Optimality

The proof of time optimality for single-input, infinite jerk (bang–bang) control profiles has been shown in the literature.[9,10] In this paper, the approach is presented for multi-input systems. First, the proof of time optimality will be outlined for multi-input, infinite jerk control sequences. Thereafter, the extension to jerk limited control profiles will be shown.

For a multi-input system in first-order form

$$\dot{\boldsymbol{x}}(t) = Q\boldsymbol{x}(t) + R\boldsymbol{u}(t), \qquad |u_k(t)| \leq 1 \qquad \forall\, k \in \{1, 2, \dots, p\}$$
$$Q \in \mathcal{R}^{n \times n}, \qquad R \in \mathcal{R}^{n \times p} \tag{35}$$

the optimal control input is given as

$$\boldsymbol{u}(t) = -\text{sgn}[R^T \boldsymbol{\lambda}(t)] \tag{36}$$

where $\text{sgn}(\boldsymbol{x})$ is the vector signum function, which is evaluated componentwise as

$$x = \begin{bmatrix} x_1 \\ x_2 \\ \vdots \end{bmatrix} \longrightarrow \text{sgn}(\boldsymbol{x}) = \begin{bmatrix} \text{sgn}(x_1) \\ \text{sgn}(x_2) \\ \vdots \end{bmatrix} \tag{37}$$

Then, $\boldsymbol{\lambda}(t)$ is the costate vector and is the solution of the costate equation

$$\dot{\boldsymbol{\lambda}}(t) = -Q^T \boldsymbol{\lambda}(t) \Rightarrow \boldsymbol{\lambda}(t) = e^{-Q^T t} \boldsymbol{\lambda}(0) \tag{38}$$

In the following, R_k will denote the kth column of the input distribution matrix. The product

$$R_k^T \boldsymbol{\lambda}(t) = R_k^T e^{-Q^T t} \boldsymbol{\lambda}(0) \tag{39}$$

is the kth component of the switching function and must be zero for all switching times in the kth input. Therefore, $\lambda(0)$ must be in the null space of the $(n-1) \times n$ matrix P given as

$$P = \begin{bmatrix} R_1^T e^{-Q^T T_{1,1}} \\ R_1^T e^{-Q^T T_{1,2}} \\ \vdots \\ R_1^T e^{-Q^T T_{1,j}} \\ \vdots \\ R_2^T e^{-Q^T T_{2,1}} \\ R_2^T e^{-Q^T T_{2,2}} \\ \vdots \\ R_2^T e^{-Q^T T_{2,j}} \\ \vdots \\ R_i^T e^{-Q^T T_{i,1}} \\ R_i^T e^{-Q^T T_{i,2}} \\ \vdots \\ R_i^T e^{-Q^T T_{i,j}} \\ \vdots \end{bmatrix} \tag{40}$$

An arbitrary combination of entries can be selected to construct the matrix P of the appropriate size. Then $\lambda(0)$ can be solved for after all switching times have been calculated. For a time-optimal control sequence, all switches have to coincide with zero crossings of the components of the switching function.

This aforementioned approach has to be modified to account for finite limits on the jerk. Equation (36) can no longer be satisfied because the signum function is discontinuous at 0 and violates Eq. (3). Pontryagin's maximum principle states that the Hamiltonian

$$H(t) = 1 + \boldsymbol{\lambda}^T(t)[Q\boldsymbol{x}(t) + R\boldsymbol{u}(t)] \tag{41}$$

must always be made as small as possible. Because $u(t)$ is the control variable, the magnitude of the individual components of $u(t)$ must be chosen as large as possible, whereas the sign of those components is determined by the sign of the components of $\lambda^T(t)R$. Between the zero crossings, determined by the switching curve, $u(t)$ has to increase or decrease with the maximum possible time rate of change as allowed by Eq. (3). Under the constraints imposed in this paper, the time-optimal solution can only be the ramp profile.

The aforementioned technique for testing time optimality of unconstrained control profiles will now be adapted to the jerk limited case. It is exclusively used for nonsaturating control profiles, that is, $|u_k(t)| < 1\ \forall\, t$, for which the bounds on $u_k(t)$ can be neglected. For jerk limited control profiles, the time rate of change of the control inputs is constrained by

$$|\dot{u}_k(t)| \leq J \tag{42}$$

To generate these jerk limited control profiles, the system had to be augmented with an integrator in each input path. These integrators will now be treated as part of the system itself and, thus, become part of the augmented state-space matrix $\bar{Q}$. This new state-space matrix $\bar{Q}$ can be written as

$$\bar{Q} = \begin{bmatrix} Q_{n \times n} & R_{n \times p} \\ 0_{p \times n} & 0_{p \times p} \end{bmatrix} \tag{43}$$

The augmented input distribution matrix $\bar{R}$ is given as

$$\bar{R} = J \begin{bmatrix} 0_{n \times p} \\ I_{p \times p} \end{bmatrix} \tag{44}$$

For this augmented system, the input $\bar{u}_k(t)$ is restricted by $|\bar{u}_k(t)| \leq 1$. Thus, the aforementioned time-optimality proof for multi-input control sequences can be utilized.

E. Determination of the Ideal Filter Length

If the control sequence for a given input is parameterized with more switches than actually necessary to satisfy all constraint equations, some of the switches will collapse and can be removed from the control sequence. This way, the determination of the ideal filter length is already part of the design of the control sequences. However, if a more formal approach is desired, a branch and bound algorithm is suggested because the problem of allocating switches is a pure integer problem. For all nonsaturating control profiles, time optimality can be tested using Pontryagin's principle as was shown in Sec. IV.D. The branch and bound algorithm would adjust the number of switches until the time-optimal solution has been found. The time-optimal filter is the filter with the shortest response and, thus, the filter with the least number of switches that still satisfies all constraints derived earlier in this section. For nonsaturating control profiles, the test for time optimality is unfortunately very complex. In this case, the branch and bound algorithm would adjust the number of switches as long as the solution contains collapsed switches.

F. Desensitization

In this section, robustness issues are addressed. For single-input systems, Singh and Vadali[10] proposed to place multiple zeros on top of each pole of the system. The approach can be motivated by looking at the complex Taylor series expansion of $G(s)$. The expansion of the transfer function around the point s_0 in the s domain is given as

$$G(s) = \sum_{l=0}^{\infty} \frac{1}{l!} \frac{\partial^l G(s)}{\partial s^l}\bigg|_{s=s_0} (s - s_0)^l$$

$$= G(s)|_{s=s_0} + \frac{\partial G(s)}{\partial s}\bigg|_{s=s_0} (s - s_0) + \mathcal{H}OT^2(s) \tag{45}$$

where $(\partial^0/\partial s^0)G(s) = G(s)$ and $\mathcal{H}OT^2(s)$ denotes the higher-order terms of order two and higher.

As was mentioned in Sec. IV.B, placing n zeros at s_0 is equivalent to forcing $G(s)$ and the first $(n-1)$ partial derivatives of $G(s)$ with respect to s to zero at s_0. $G(s)$ and these first $(n-1)$ partial derivatives evaluated at s_0 determine the first n coefficients of the Taylor series expansion as shown in Eq. (45). Provided that the first n coefficients are zero, then the magnitude of the transfer function grows with the nth power of $(s - s_0)$ and rises slower for larger n in the vicinity of s_0.

The requirement that the lth partial derivative of $G_{F,i}(s)$ with respect to s has to be zero at $s = \pm j\omega_i$ is written as

$$\frac{\partial^l}{\partial s^l} G_{F,i}(s)|_{s=\pm j\omega_i} = 0 \tag{46}$$

To place a total of L conjugate complex pairs of zeros on top of the conjugate complex pair of poles corresponding to the ith mode, a total of $2L-2$ additional constraint equations has to be satisfied. This set is given as

$$\begin{bmatrix} \sum_{k=1}^{p} D_{i,k} \left(\sum_{j=1}^{n_k} A_{k,j} (-T_{k,j})^l \cos(\omega_i T_{k,j}) \right) = 0 \\ \sum_{k=1}^{p} D_{i,k} \left(\sum_{j=1}^{n_k} A_{k,j} (-T_{k,j})^l \sin(\omega_i T_{k,j}) \right) = 0 \end{bmatrix}$$

$$\forall\, l \in \{1, \ldots, (L-1)\} \tag{47}$$

The case $L = 0$ has been removed from this set of constraints because it is already covered in Eq. (26). The number of switches in the input sequences has to be increased accordingly to account for the additional constraints.

V. Numerical Examples

The example presented in this section deals with the design of control sequences for a three-mass/two-spring system, as shown in Fig. 3. This system has the dynamics

$$\begin{bmatrix} m_1 & 0 & 0 \\ 0 & m_2 & 0 \\ 0 & 0 & m_3 \end{bmatrix} \begin{bmatrix} \ddot{y}_1(t) \\ \ddot{y}_2(t) \\ \ddot{y}_3(t) \end{bmatrix} + \begin{bmatrix} k_1 & -k_1 & 0 \\ -k_1 & k_1 + k_2 & -k_2 \\ 0 & -k_2 & k_2 \end{bmatrix} \begin{bmatrix} y_1(t) \\ y_2(t) \\ y_3(t) \end{bmatrix}$$

$$= \begin{bmatrix} 1 & 0 \\ 0 & 0 \\ 0 & 1 \end{bmatrix} \begin{bmatrix} u_1(t) \\ u_2(t) \end{bmatrix} \tag{48}$$

For all examples in this section, the parameters of the system have been chosen as

$$m_1 = 1 \qquad m_2 = 2 \qquad m_3 = \tfrac{1}{2} \qquad k_1 = 1 \qquad k_2 = 1 \tag{49}$$

so that

$$\omega_1 = 1.1371 \text{ rad/s} \qquad \omega_2 = 1.6453 \text{ rad/s} \tag{50}$$

are the natural frequencies of the two oscillatory modes.

A. Simulation Results

A jerk limited/time-optimal control profile has been designed for a maximum allowable jerk of $J = 1$ to illustrate the design technique. The switching curves have also been provided to prove time optimality.

The resulting set of control sequences is given as

$$u_1(t) = 1(\langle t \rangle - 2\langle t - 0.7404 \rangle + 2\langle t - 1.9859 \rangle - 2\langle t - 2.9964 \rangle$$
$$+ 2\langle t - 4.2420 \rangle - \langle t - 4.9823 \rangle) \tag{51}$$

$$u_2(t) = 1(\langle t \rangle - 2\langle t - 0.7723 \rangle + 2\langle t - 2.0179 \rangle - 2\langle t - 2.9644 \rangle$$
$$+ 2\langle t - 4.2100 \rangle - \langle t - 4.9823 \rangle) \tag{52}$$

where $\langle x \rangle = x\mathcal{H}(x)$. The final time is 4.9823 s. Figure 4 shows the system response and the control input. As can be seen from Fig. 4, this example presents a nonsaturating control profile, that is, Eq. (3) prevented the control from saturating. The proof of time optimality has been provided in Fig. 5, which plots the components of the switching function along with the control sequences.

B. Trajectories of the Switching Times

In this section, the change in the structure of the control profiles for different limits on the maximum allowable jerk J is illustrated. The trajectories of the switching times are shown in Fig. 6 for the first input and Fig. 7 for the second input. Figures 6 and 7 summarize the results of the design process for a region of bounds on jerk ranging from 0.15 to 800. In both diagrams, the abscissa represents the maximum allowable amount of jerk, whereas the ordinate corresponds to the switching times. The thick vertical lines mark transitions, that is, discrete values of jerk for which the control profile changes its overall shape. The small boxes inserted into Figs. 6 and 7 plot the overall shape of the control profiles in the different regions. The

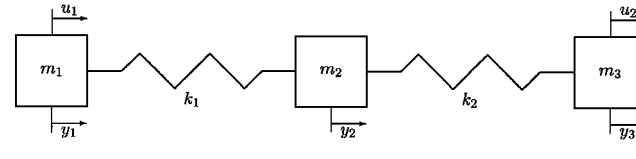

Fig. 3 Three-mass/two-spring multi-input system.

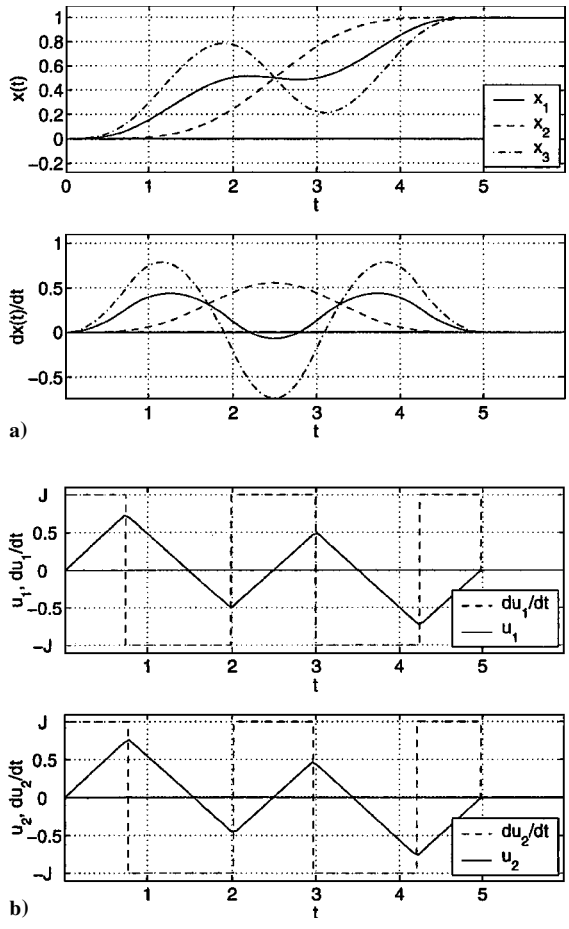

Fig. 4 $J = 1$: a) system response and b) control profiles.

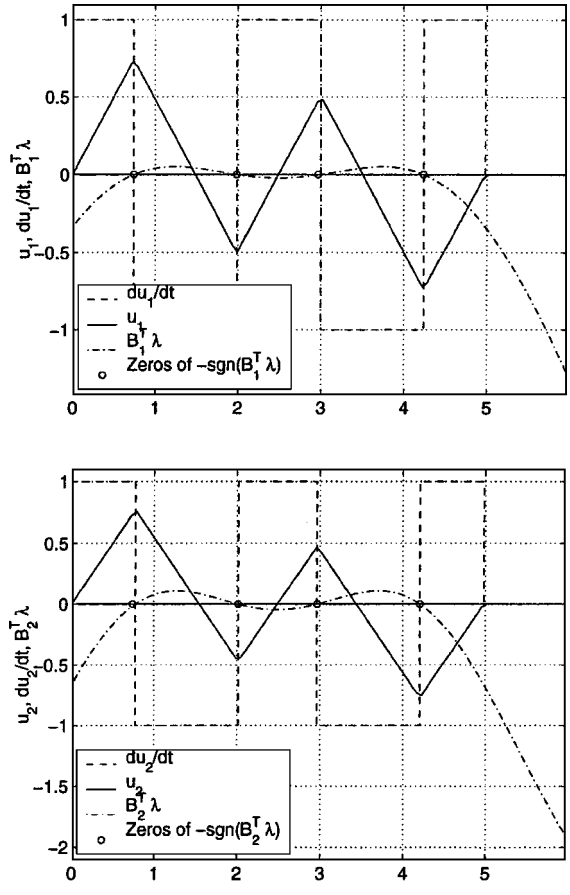

Fig. 5 Switching curves for both system inputs ($J = 1$).

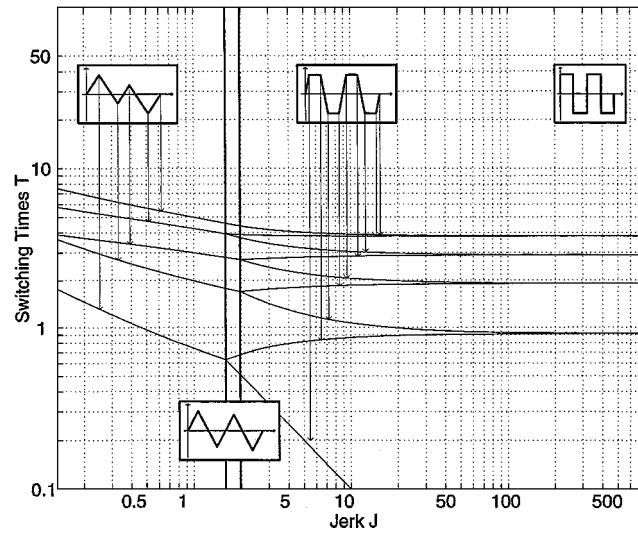

Fig. 6 Trajectories of the switching times ($J \in [0.15, 800]$, input 1).

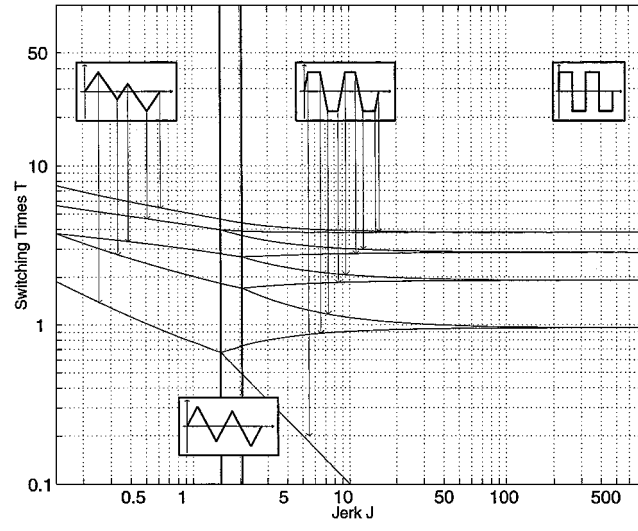

Fig. 7 Trajectories of the switching times ($J \in [0.15, 800]$, input 2).

vertical arrows establish a connection between the trajectories and the switching times.

The exact locations of the transitions are given as $J = 1.5855$ and 1.9635 for the first input, as well as $J = 1.5005$ and 2.0560 for the second input. At those points, one can see that two trajectories coincide, meaning that two switches will take place at the same instant in time.

In addition, this diagram also provides means to compare the maneuver time for different magnitudes of the maximum allowable amount of jerk. The topmost curve shows the maneuver time. On reducing the maximum amount of jerk from 800 to 8, that is, by a factor of 100, the maneuver increases from 3.8109 to 3.9399. The jerk constraint of 800 has a solution that is nearly coincident with the time-optimal control, permitting us to compare the jerk constrained solution to the time-optimal solution.

C. Robustness Toward Parameter Deviations

In this example, the effect of placing additional zeros at the oscillatory modes is illustrated. Control profiles for an arbitrarily chosen maximum permissible jerk of $J = 1.4$ will be compared. The first pair of profiles places one zero at each oscillatory pole. These sequences are given as

$$u_1(t) = 1.4(t - 2\langle t - 0.6576\rangle + 2\langle t - 1.8272\rangle - 2\langle t - 2.8510\rangle + 2\langle t - 4.0205\rangle - \langle t - 4.6782\rangle) \quad (53)$$

$$u_2(t) = 1.4(t - 2\langle t - 0.6828\rangle + 2\langle t - 1.8524\rangle - 2\langle t - 2.8258\rangle + 2\langle t - 3.9954\rangle - \langle t - 4.6782\rangle) \quad (54)$$

resulting in a maneuver duration of 4.6782 s. The pair of sequences

$$u_1(t) = 1.4(t - 2\langle t - 0.4980\rangle + 2\langle t - 1.4154\rangle - 2\langle t - 2.4492\rangle + 2\langle t - 3.6780\rangle - 2\langle t - 4.7119\rangle + 2\langle t - 5.6294\rangle - \langle t - 6.1274\rangle) \quad (55)$$

and

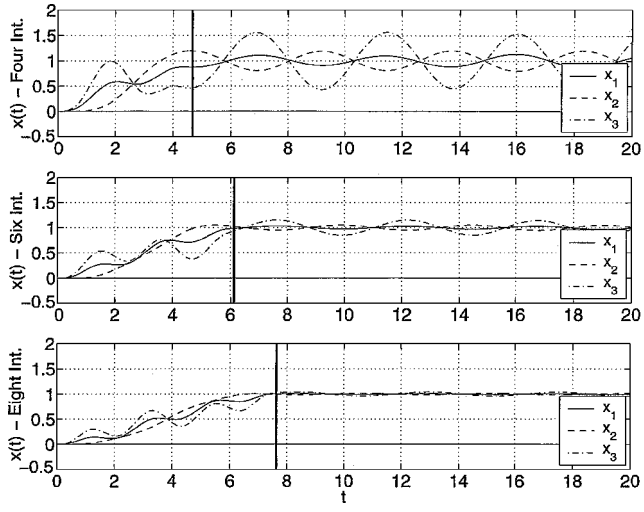

Fig. 8 System responses for nonnominal spring stiffness $k_1 = k_2 = 0.7$ and added robustness constraints.

$$u_2(t) = 1.4(t - 2\langle t - 0.5246\rangle + 2\langle t - 1.4458\rangle - 2\langle t - 2.4531\rangle + 2\langle t - 3.6743\rangle - 2\langle t - 4.6816\rangle + 2\langle t - 5.6028\rangle - \langle t - 6.1274\rangle) \quad (56)$$

places two zeros on top of each oscillatory pole and has a final time of 6.1274 s. The two control sequences

$$u_1(t) = 1.4(t - 2\langle t - 0.3918\rangle + 2\langle t - 1.1759\rangle - 2\langle t - 2.1694\rangle + 2\langle t - 3.2935\rangle - 2\langle t - 4.3395\rangle + 2\langle t - 5.4637\rangle - 2\langle t - 6.4572\rangle + 2\langle t - 7.2413\rangle - \langle t - 7.6331\rangle) \quad (57)$$

and

$$u_2(t) = 1.4(t - 2\langle t - 0.4143\rangle + 2\langle t - 1.2087\rangle - 2\langle t - 2.1973\rangle + 2\langle t - 3.3112\rangle - 2\langle t - 4.3219\rangle + 2\langle t - 5.4358\rangle - 2\langle t - 6.4244\rangle + 2\langle t - 7.2188\rangle - \langle t - 7.6331\rangle) \quad (58)$$

provide even more robustness toward errors in the system parameters because three pairs of zeros are placed on top of each oscillatory pair of poles. Completion of this maneuver takes 7.6331 s. Figure 8 shows the response of the three- mass/two-spring system for a nonnominal spring stiffness $k_1 = k_2 = 0.7$. This rather large deviation from the nominal value of $k_1 = k_2 = 1$ was chosen to demonstrate clearly the effect of the added robustness constraints on the system response.

From top to bottom, Fig. 8 shows three profiles with more and more focus on robustness toward parametric uncertainties. The first profile has been designed without adding constraints for increased robustness, that is, Eq. (47) is not added to the set of constraints. Although this profile will inhibit residual vibration for the nominal case ($k_1 = k_2 = 1$), the control performance drops considerably for

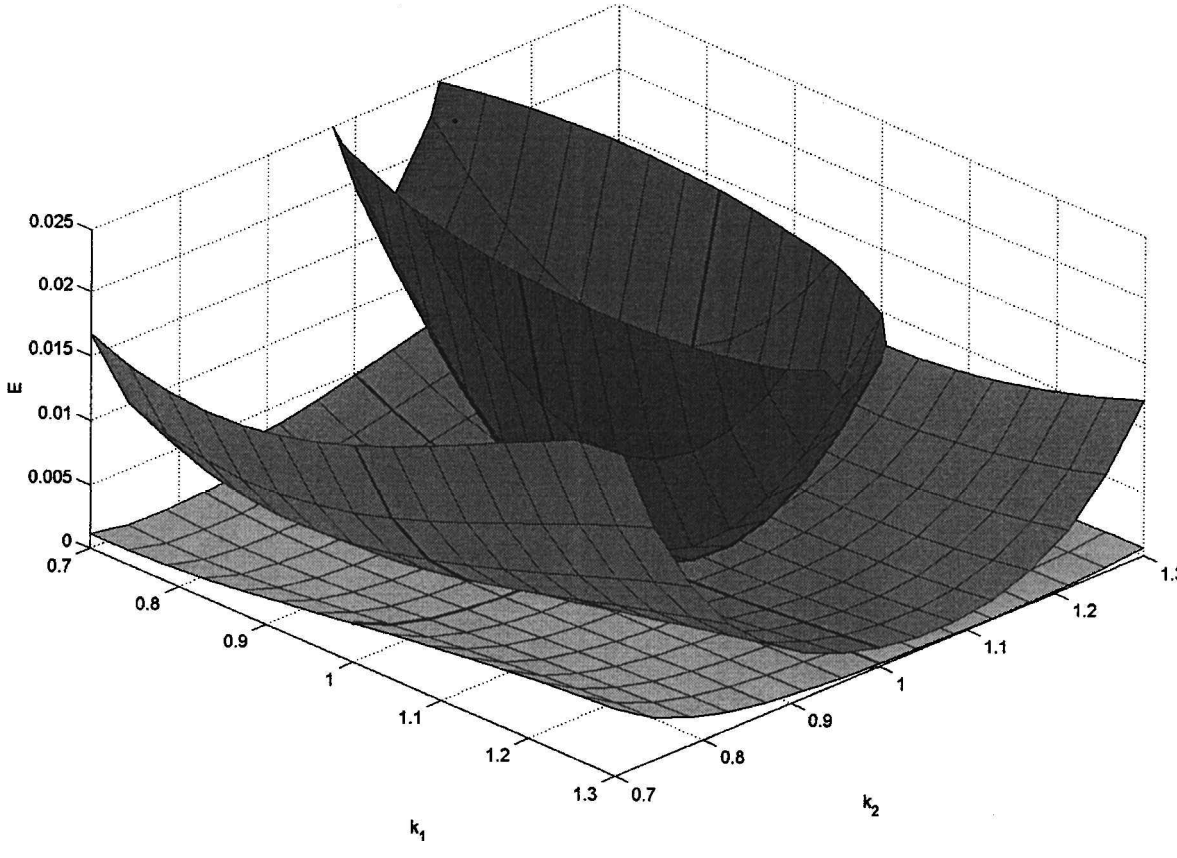

Fig. 9 Cost surfaces (residual energy over uncertain parameters).

the nonnominal case presented in Fig. 8. It can be seen that the system has not come to rest at the final time and still exhibits residual vibration. The next profile has one set of robustness constraints added, that is, $L = 1$ [Eq. (47)]. The third profile has been designed with $L = 2$ and is even more robust to the parametric uncertainty. A measure for residual vibration is the amount of energy stored in the system at the final time. The total energy stored in the system at the final time is given as

$$E = \tfrac{1}{2}\dot{y}^T(T_{\text{final}})M\dot{y}(T_{\text{final}}) + \tfrac{1}{2}y^T(T_{\text{final}})Ky(T_{\text{final}}) \qquad (59)$$

The residual energy of the three profiles from top to bottom has been calculated as

$$E_1 = 0.2281 \qquad E_2 = 0.0167 \qquad E_3 = 0.0012 \qquad (60)$$

for the parameter set $k_1 = k_2 = 0.7$. The final time of each control profile is marked with a vertical line. Note how maneuver time has been traded for robustness.

To illustrate the improved performance of the desensitized controllers, the residual energy is plotted for the uncertain domain, as shown in Fig. 9. From top to bottom, the three surfaces denote the nonrobust ($L = 0$) and two robust ($L = 1, 2$) cases, respectively. The thick lines on the surface denote the nominal model parameters. The improvement in performance is evident from Fig. 9.

VI. Conclusions

The design of jerk limited control sequences for multi-input systems was presented in this paper. The design of these sequences was posed as a pole-cancellation problem. The filters for all system inputs are designed simultaneously, which improves control performance compared to the case where each input prefilter is designed separately. Analytical expressions have been derived that permit the easy evaluation of the filter coefficients. Pontryagin's principle has been adapted to multi-input systems and has been used to test for time optimality of all nonsaturating profiles. Robustness can be increased by placing multiple zeros on top of the oscillatory poles of the plant. It has been shown that robustness increases with the number of zeros placed on top of the system poles. The proposed technique has been applied to a three-mass/two-spring system to illustrate the results and can be extended to damped systems. This requires that the zeros of the filter be placed at the estimated locations of the damped poles.

References

[1] Junkins, J. L., Rahman, Z., and Bang, H., "Near-Minimum Time Maneuvers of Flexible Vehicles: A Liapunov Control Law Design Method," *Mechanics and Control of Large Flexible Structures*, AIAA, Washington, DC, 1990, pp. 565–593.

[2] Ballhaus, W. L., Rock, S. M., and Bryson, A. E., "Optimal Control of a Two-Link Flexible Robotic Manipulator Using Time-Varying Controller Gains," American Astronautical Society, AAS Paper 92-055, 1992.

[3] Bhat, S. P., and Miu, D. K., "Minimum Power and Minimum Jerk Control and Its Application in Computer Disk Drives," *IEEE Transactions on Magnetics*, Vol. 27, No. 6, 1991, pp. 4471–4475.

[4] Singhose, W. E., Porter, L. J., and Seering, W. P., "Input Shaped Control of a Planar Gantry Crane with Hoisting," *Proceedings of the American Control Conference*, IEEE Publ., Piscataway, NJ, 1997, pp. 97–100.

[5] Smith, O. J. M., "Posicast Control of Damped Oscillatory Systems," *Proceedings of the IRE*, Vol. 45, 1957, pp. 1249–1255.

[6] Singer, N. C., and Seering, W. P., "Preshaping Command Inputs to Reduce System Vibrations," *Journal of Dynamic Systems, Measurement and Control*, Vol. 112, No. 1, 1990, pp. 76–82.

[7] Singh, T., and Vadali, S. R., "Robust Time-Delay Control," *Journal of Dynamic Systems, Measurement and Control*, Vol. 115, No. 2(A), 1993, pp. 303–306.

[8] Singhose, W. E., Porter, L. J., and Singer, N. P., "Vibration Reduction Using Multi-Hump Extra-Insensitive Input Shapers," *Proceedings of the American Control Conference*, IEEE Publ., Piscataway, NJ, 1995, pp. 3830–3834.

[9] Liu, Q., and Wie, B., "Robust Time-Optimal Control of Uncertain Flexible Spacecraft," *Journal of Guidance, Control, and Dynamics*, Vol. 15, No. 3, 1992, pp. 597–604.

[10] Singh, T., and Vadali, S. R., "Robust Time-Optimal Control: Frequency Domain Approach," *Journal of Guidance, Control, and Dynamics*, Vol. 17, No. 2, 1994, pp. 346–353.

[11] Singh, T., "Minimax Design of Robust Controllers for Flexible Structures," *Journal of Guidance, Control, and Dynamics* (submitted for publication).

[12] Hindle, T. A., and Singh, T., "Robust Minimum Power/Jerk Control of Maneuvering Structures," *Journal of Guidance, Control, and Dynamics*, Vol. 24, No. 4, 2001, pp. 316–326.

[13] Singh, T., and Vadali, S. R., "Robust Time-Delay Control of Multimode Systems," *International Journal of Control*, Vol. 62, No. 6, 1995, pp. 1319–1339.

[14] Lim, S., Stevens, H. D., and How, J. P., "Input Shaping Design for Multi-Input Flexible Systems," *Journal of Dynamic Systems, Measurement and Control*, Vol. 121, No. 3, 1991, pp. 443–447.

[15] Pao, L. Y., "Input Shaping Design for Flexible Systems with Multiple Actuators," *Proceedings of the 13th World Congress of the International Federation of Automatic Control*, Elsevier Science, New York, 1996, pp. 267–272.